Aerospace Science and Technology 43 (2015) 236–244

Contents lists available at ScienceDirect

Aerospace Science and Technology

www.elsevier.com/locate/aescte

Modeling and analysis of dynamics for spacecraft relative motion actuated by inter-satellite non-contacting force

Yuan-wen Zhang *, Le-ping Yang, Yan-wei Zhu, Huan Huang, Wei-wei Cai

National University of Defense Technology, Changsha, Hunan 410073, PR China

ARTICLE INFO

Article history:
Received 1 February 2013
Received in revised form 29 April 2013
Accepted 5 March 2015
Available online 14 March 2015

Keywords:
Spacecraft relative motion
Inter-satellite non-contacting force
Unified modeling
Dynamic model
Dynamics analysis

ABSTRACT

With the recent flurry of research on spacecraft relative motion actuated by inter-satellite non-contacting force, i.e., electrostatic force, electromagnetic force and magnetic flux-pinned force, the need has become apparent for dynamic modeling and dynamics analysis that capture the characteristics of this generic force. Based on the basic derivation of electrostatic force model and some theorems, the actuations of electrostatic force, electromagnetic force/torque and magnetic flux-pinned force/torque are unified and the corresponding mathematic models are derived. And then, with a general notation of this inter-satellite non-contacting force, the dynamic models are developed with respect to several assumptions of circular orbit, elliptical orbit and general Keplerian orbit pertaining to the motion of center of mass of the spacecraft cluster. A detailed dynamics analysis based on these derived models are carried out, including constraints of the relative motion dynamics, the special characteristics of applications to the near-Earth relative orbit motion and the deep space relative motion, and then a case with co-rotating pair of satellites subject to the previously mentioned inter-satellite non-contacting forces was simulated to validate the dynamic modeling and dynamics analysis. At last, some useful conclusions follow.

1. Introduction

The actuation force for spacecraft operation can be classified to three categories: the independent thruster force [1] acting on individual spacecraft, the inter-satellite contacting force [2,3] and the inter-satellite non-contacting force [4–7] acting on all the relevant spacecraft. Compared to the first actuation force, the third one has advantages of fuel-efficiency, cleanness, simultaneous and distant actuation. Specifically, as to the spacecraft cluster missions, the relative motion between spacecraft, instead of the absolute inertial motion in space, is important. However, thruster force actuates inertial degrees-of-freedom, while the inter-satellite non-contacting force actuates relative degrees-of-freedom. Compared to the second actuation force, the third one has advantages of higher safety, more degrees-of-freedom for relative motion and mission operations. Therefore, the inter-satellite non-contacting force has attracted more and more attention in the research field recently.

Nowadays, the three mainly studied inter-satellite non-contacting forces are the electrostatic force, the electromagnetic force and the magnetic flux-pinned force. Although their actuation principles are different, it is actually true that they share several similar characteristics. For example, they all belong to field force, and being narrow range but high control precision. Schweighart has proven that the far-field electromagnetic force/torque models are equal to the mathematical models produced by two sets of charge, each of which includes a $+q$ and a $-q$ separated by a distance [8]. In addition, Wilson et al. [9], Jones and Peck [10] have verified that the actuation effect of magnetic flux-pinned force could be empirically represented by the interactions of the actual magnetic field with the "frozen magnetic dipole" created in response to the field source's position at the time of cooling and the "mobile magnetic dipole" that changes position as the actual magnetic field source moves. Therefore, based on this representation and the electrostatic/magnetostatic duality theorem, there is a possibility of unifying the mathematical modeling of the three forces.

With the development of space operation technology, such as formation flight, rendezvous and docking, fractionated spacecraft and on-orbit servicing, relative motion dynamics of spacecraft has become a hot research topic and the main mission implementation mode. To date, many modeling approaches of the spacecraft relative motions enabled by inter-satellite non-contacting force are based on the Hill equations, which are linear and convenient for dynamics analysis and controller design [11]. However, the Hill equations are only valid for circular reference orbit and small relative distance between the spacecraft, which poses limitations on the applications to other kinds of conic-section reference orbit mo-

* Corresponding author. Tel.: +86 13637479241.
E-mail address: pointmaker8384@126.com (Y.-w. Zhang).

http://dx.doi.org/10.1016/j.ast.2015.03.003
1270-9638/

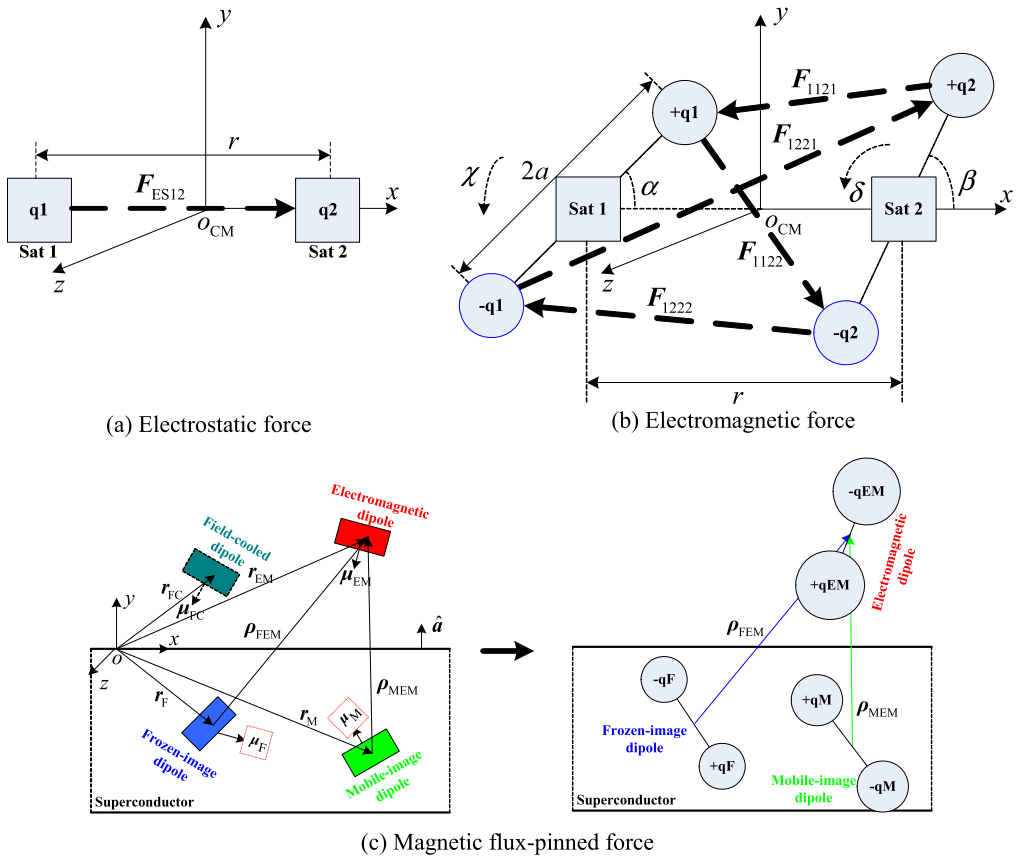

Fig. 1. General formulation of the three inter-satellite non-contacting forces.

tion. In addition, the relative attitude dynamics should also be exploited.

As these inter-satellite non-contacting forces have found more and more applications, some novel and interesting dynamics characteristics appear [12–16], which constrain the degrees-of-freedom of spacecraft relative motion. However, these dynamics characteristics have not been generally and systematically studied by far.

In this paper, based on the unified modeling of the three inter-satellite non-contacting forces, several dynamic models and dynamics analysis of spacecraft relative motion are theoretical derivation and numerical validated. Firstly, applying the electrostatic/magnetostatic duality theorem and the image-dipole representation of the magnetic flux-pinned force, the unified mathematical models of the three forces are derived. Secondly, considering several different orbit motion assumptions of the center of mass (denoted as CM) of the spacecraft cluster, including circular orbit, elliptical orbit and general Keplerian orbit, based on the equations of the Hill model, the T–H model and the orbit elements model, three corresponding relative motion dynamic models actuated by this generic inter-satellite non-contacting force are developed. Thirdly, after investigating these derived models, the constraints of relative motion dynamics, the characteristics of application to the near-Earth relative orbit motion and the deep space relative motion are analyzed in detail. Fourthly, cases with co-rotating pair of satellites subject to the three inter-satellite non-contacting forces were simulated to validate the dynamic modeling and dynamics analysis. At last, some useful conclusions are given.

2. Dynamic modeling

In this section, the mathematical models of the three inter-satellite non-contacting forces are unified, and several dynamic models of relative translational motion considering different referenced orbit assumptions are derived. In addition, the dynamic model of relative attitude motion is simply put forward.

2.1. General formulation of the three inter-satellite non-contacting forces

To deal with these dynamic problems in a unified way, we try to develop a general mathematical model for these forces. In general, the electrostatic force has the simplest formulation with respect to the other two forces, so this general mathematical model is developed on the basis of electrostatic formulation. The electrostatic force formulation for two satellites is depicted as Fig. 1(a). Based on the electrostatic/magnetostatic duality theorem [8], we utilize the electrostatics duality approach to derive the far-field electromagnetic force/torque models, depicted as Fig. 1(b). Magnetic flux-pinned force refers to the interaction between a magnetic field and a high-temperature superconductor (HTSC), which establishes an equilibrium position and orientation of the magnetic field relative to the HTSC. Based on the image-dipole model of magnetic flux-pinned force [10,17,18] and the electrostatic/magnetostatic duality theorem, we derive the multiple electrostatic forces formulation for the magnetic flux-pinned interaction, depicted as Fig. 1(c).

Therefore, based on the depictions of Fig. 1, the general formulations of the three inter-satellite non-contacting forces are derived as follows.

For electrostatic force, ignoring the Debye shielding effect, only the axis aligned force exists, which can be derived as

$$\boldsymbol{F}_{ES12} = -k_c \frac{q_1 q_2}{r^2} \hat{\boldsymbol{r}} \tag{1}$$

where $\boldsymbol{F}_{ES12}$ denotes the electrostatic force on satellite 1 actuated by satellite 2, Coulomb constant $k_c = 8.99 \times 10^9\ \mathrm{Nm^2\,C^{-2}}$, r is the

separation distance of the two satellites and $\hat{\boldsymbol{r}}$ the unit distance vector from satellite 1 to 2, q_1 and q_2 are the charges on the two satellites, and the subscript "ES" represents corresponding terms of electrostatic actuation.

For electromagnetic force, three dimensional force and torque can be produced, which is derived as

$$\begin{cases} \boldsymbol{F}_{\mathrm{EM12}}(\alpha,\beta,\chi,\delta,\boldsymbol{r},a,q_1q_2,k_c) \\ \quad = \boldsymbol{F}_{1121}+\boldsymbol{F}_{1122}+\boldsymbol{F}_{1221}+\boldsymbol{F}_{1222} \\ \tau_{\mathrm{EM12}}(\alpha,\beta,\chi,\delta,\boldsymbol{r},a,q_1q_2,k_c) \\ \quad = \boldsymbol{\tau}_{1121}+\boldsymbol{\tau}_{1122}+\boldsymbol{\tau}_{1221}+\boldsymbol{\tau}_{1222} \end{cases} \tag{2}$$

where α, χ are the two angles of the magnetic moment vector on satellite 1 with respect to and rotating with $o_{\mathrm{CM}}x$ axis, β, δ are the corresponding terms of satellite 2, and $2a$ is distance between the positive and the negative charge on the same satellite. Specifically, $\boldsymbol{F}_{1121}$ represents the electrostatic force on the positive charge of satellite 1 actuated by the positive charge on satellite 2, etc.

The electrostatic/magnetostatic duality principles are defined as

$$\begin{cases} k_c \to \mu_0/4\pi \\ q_i = \mu_i/2a \end{cases} \tag{3}$$

where μ_0 is the permeability of free space and μ_i the strength of magnetic dipole on satellite i.

For magnetic flux-pinned force, three dimensional force and torque can also be produced, which is derived as

$$\begin{cases} \boldsymbol{F}_{\mathrm{FP12}}(\alpha_1,\beta_1,\chi_1,\delta_1,\boldsymbol{\rho}_{\mathrm{FEM}},\alpha_2,\beta_2,\chi_2,\delta_2,\boldsymbol{\rho}_{\mathrm{MEM}},a,q_{\mathrm{F}}q_{\mathrm{EM}},q_{\mathrm{M}}q_{\mathrm{EM}},k_c) \\ \quad = \boldsymbol{F}_{\mathrm{EM1F1}}+\boldsymbol{F}_{\mathrm{EM1F2}}+\boldsymbol{F}_{\mathrm{EM2F1}}+\boldsymbol{F}_{\mathrm{EM2F2}}+\boldsymbol{F}_{\mathrm{EM1M1}}+\boldsymbol{F}_{\mathrm{EM1M2}} \\ \qquad +\boldsymbol{F}_{\mathrm{EM2M1}}+\boldsymbol{F}_{\mathrm{EM2M2}} \\ \tau_{\mathrm{FP12}}(\alpha_1,\beta_1,\chi_1,\delta_1,\boldsymbol{\rho}_{\mathrm{FEM}},\alpha_2,\beta_2,\chi_2,\delta_2,\boldsymbol{\rho}_{\mathrm{MEM}},a,q_{\mathrm{F}}q_{\mathrm{EM}},q_{\mathrm{M}}q_{\mathrm{EM}},k_c) \\ \quad = \boldsymbol{\tau}_{\mathrm{EM1F1}}+\boldsymbol{\tau}_{\mathrm{EM1F2}}+\boldsymbol{\tau}_{\mathrm{EM2F1}}+\boldsymbol{\tau}_{\mathrm{EM2F2}}+\boldsymbol{\tau}_{\mathrm{EM1M1}}+\boldsymbol{\tau}_{\mathrm{EM1M2}} \\ \qquad +\boldsymbol{\tau}_{\mathrm{EM2M1}}+\boldsymbol{\tau}_{\mathrm{EM2M2}} \end{cases} \tag{4}$$

where $q_{\mathrm{F}}, q_{\mathrm{M}}, q_{\mathrm{EM}}$ are defined as

$$q_{\mathrm{F}} = \mu_{\mathrm{F}}/2a, \qquad q_{\mathrm{M}} = \mu_{\mathrm{M}}/2a, \qquad q_{\mathrm{EM}} = \mu_{\mathrm{EM}}/2a \tag{5}$$

The magnetic moment vectors $\boldsymbol{\mu}_{\mathrm{F}}, \boldsymbol{\mu}_{\mathrm{M}}$ are derived as

$$\begin{cases} \boldsymbol{\mu}_{\mathrm{F}} = 2(\hat{\boldsymbol{a}}\cdot\boldsymbol{\mu}_{\mathrm{FC}})\hat{\boldsymbol{a}} - \boldsymbol{\mu}_{\mathrm{FC}} \\ \boldsymbol{\mu}_{\mathrm{M}} = \boldsymbol{\mu}_{\mathrm{EM}} - 2(\hat{\boldsymbol{a}}\cdot\boldsymbol{\mu}_{\mathrm{EM}})\hat{\boldsymbol{a}} \end{cases} \tag{6}$$

where $\hat{\boldsymbol{a}}$ is the unit orientation vector of the superconductor surface.

The angles $\alpha_1, \beta_1, \chi_1, \delta_1$ and $\alpha_2, \beta_2, \chi_2, \delta_2$ have similar definitions as $\alpha, \beta, \chi, \delta$ about the axes connecting the "Frozen-image dipole" and the "Electromagnetic dipole", the "Mobile-image dipole" and the "Electromagnetic dipole", respectively. The relative distance vectors $\boldsymbol{\rho}_{\mathrm{FEM}}, \boldsymbol{\rho}_{\mathrm{MEM}}$ are derived as

$$\begin{cases} \boldsymbol{\rho}_{\mathrm{FEM}} = \boldsymbol{r}_{\mathrm{EM}} - \boldsymbol{r}_{\mathrm{FC}} + 2(\hat{\boldsymbol{a}}\cdot\boldsymbol{r}_{\mathrm{FC}})\hat{\boldsymbol{a}} \\ \boldsymbol{\rho}_{\mathrm{MEM}} = 2(\hat{\boldsymbol{a}}\cdot\boldsymbol{r}_{\mathrm{EM}})\hat{\boldsymbol{a}} \end{cases} \tag{7}$$

2.2. Dynamic models of relative translational motion

With application of this generic inter-satellite non-contacting force, the interaction between the translational motion and the attitude motion is depicted as Fig. 2. Before deriving the dynamic models, the related reference frames and coordinates are firstly defined and depicted as Fig. 3. The frame $O_{\mathrm{E}}X_{\mathrm{I}}Y_{\mathrm{I}}Z_{\mathrm{I}}$ is the ECI frame and $o_{\mathrm{CM}}xyz$ the Hill frame at the CM. And, $\boldsymbol{R}_i$, $\boldsymbol{R}_j$, $\boldsymbol{R}_{\mathrm{CM}}$ are the distance vectors of satellites i, j and CM with respect to the center of the Earth. Additionally, $\boldsymbol{r}_i, \boldsymbol{r}_j$ are the relative distance vectors of satellite i and j with respect to CM, and $\boldsymbol{r}_{ij}$ is the relative distance vector from satellite i to j.

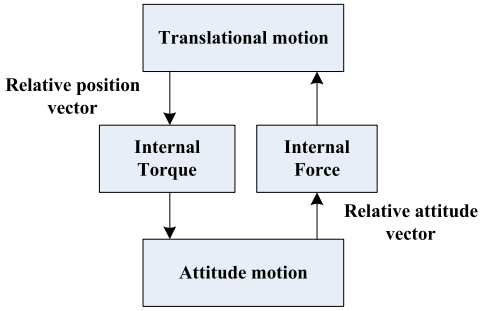

Fig. 2. Coupled interaction between the translational and the attitude motion.

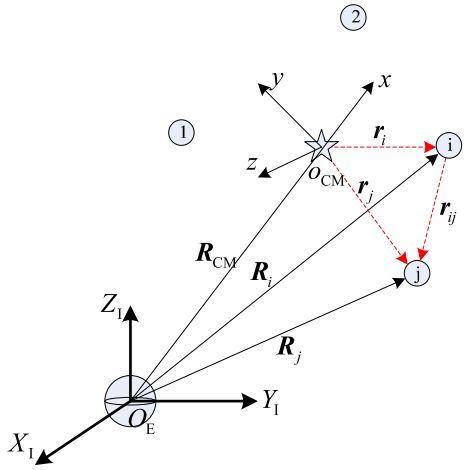

Fig. 3. Related reference frames and coordinates.

We choose relative positions $(x, y, z)^{\mathrm{T}}$ and attitudes $(\varphi, \theta, \psi)^{\mathrm{T}}$ with respect to the Hill frame at CM as system states of the spacecraft cluster, denoted as

$$\boldsymbol{X} = [x_1, y_1, z_1, \ldots x_N, y_N, z_N, \varphi_1, \theta_1, \psi_1, \ldots, \varphi_N, \theta_N, \psi_N]^{\mathrm{T}} \tag{8}$$

where N is the number of satellites in the cluster.

1) CM with circular orbit.

When CM with circular orbit is assumed, the Hill equations can be utilized. With the continuous actuation of inter-satellite non-contacting force, the orbit motions of all satellites actually are non-Keplerian orbit, therefore the Hill frame at CM is chosen as the reference frame. Based on the Hill equations, the dynamic model of relative translational motion for satellite i with respect to CM is directly developed as

$$\begin{cases} \ddot{x}_i - 2n_{\mathrm{CM}}\dot{y}_i - 3n_{\mathrm{CM}}^2 x_i = \sum\limits_{k=1,k\neq i}^{N} f_{xk}^i(\boldsymbol{X}) \\ \ddot{y}_i + 2n_{\mathrm{CM}}\dot{x}_i = \sum\limits_{k=1,k\neq i}^{N} f_{yk}^i(\boldsymbol{X}) \\ \ddot{z}_i + n_{\mathrm{CM}}^2 z_i = \sum\limits_{k=1,k\neq i}^{N} f_{zk}^i(\boldsymbol{X}) \end{cases} \tag{9}$$

where n_{CM} is the orbit speed of CM, (x_i, y_i, z_i) are the projections of $\boldsymbol{r}_i$ in $o_{\mathrm{CM}}xyz$, $(f_{kx}^i, f_{ky}^i, f_{kz}^i)$ are the projections of the specific inter-satellite non-contacting force of satellite i actuated by satellite k.

Incorporating the relationship of $\boldsymbol{r}_{ij} = \boldsymbol{r}_j - \boldsymbol{r}_i$, the dynamic model of relative motion for satellite j with respect to satellite i is derived as

$$\begin{cases} \ddot{x}_{ij} - 2n_{\mathrm{CM}}\dot{y}_{ij} - 3n_{\mathrm{CM}}^2 x_{ij} = \sum\limits_{k=1,k\neq j}^{N} f_{xk}^{j}(\boldsymbol{X}) - \sum\limits_{k=1,k\neq i}^{N} f_{xk}^{i}(\boldsymbol{X}) \\ \ddot{y}_{ij} + 2n_{\mathrm{CM}}\dot{x}_{ij} = \sum\limits_{k=1,k\neq j}^{N} f_{yk}^{j}(\boldsymbol{X}) - \sum\limits_{k=1,k\neq i}^{N} f_{yk}^{i}(\boldsymbol{X}) \\ \ddot{z}_{ij} + n_{\mathrm{CM}}^2 z_{ij} = \sum\limits_{k=1,k\neq j}^{N} f_{zk}^{j}(\boldsymbol{X}) - \sum\limits_{k=1,k\neq i}^{N} f_{zk}^{i}(\boldsymbol{X}) \end{cases} \tag{10}$$

where x_{ij}, y_{ij}, z_{ij} are the projections of $\boldsymbol{r}_{ij}$ in $o_{\mathrm{CM}}xyz$.

To sum up, regardless of whether the orbital motions of the satellites are circular, as long as the hypothesis of circular orbit for CM is valid, the dynamic models of relative motion for arbitrary satellite with respect to CM and the other satellites can be derived as Eq. (9) and (10) respectively.

2) CM with elliptical orbit.

When CM with elliptical orbit is assumed, the T–H equations can be utilized [19]. Based on the same reference frame chosen of the above case and the T–H model, the dynamic model of relative translational motion for satellite i with respect to CM is directly derived as

$$\begin{cases} x_i'' - \dfrac{2e\sin\theta}{1+e\cos\theta}x_i' - 2y_i' - \dfrac{3+e\cos\theta}{1+e\cos\theta}x_i + \dfrac{2e\sin\theta}{1+e\cos\theta}y_i \\ \quad = \dfrac{(1-e^2)^3}{n_{\mathrm{CM}}^2(1+e\cos\theta)^4}\sum\limits_{k=1,k\neq i}^{N} f_{xk}^{i}(\boldsymbol{X}) \\ y_i'' + 2x_i' - \dfrac{2e\sin\theta}{1+e\cos\theta}y_i' - \dfrac{2e\sin\theta}{1+e\cos\theta}x_i - \dfrac{e\cos\theta}{1+e\cos\theta}y_i \\ \quad = \dfrac{(1-e^2)^3}{n_{\mathrm{CM}}^2(1+e\cos\theta)^4}\sum\limits_{k=1,k\neq i}^{N} f_{yk}^{i}(\boldsymbol{X}) \\ z_i'' - \dfrac{2e\sin\theta}{1+e\cos\theta}z_i' + \dfrac{1}{1+e\cos\theta}z_i \\ \quad = \dfrac{(1-e^2)^3}{n_{\mathrm{CM}}^2(1+e\cos\theta)^4}\sum\limits_{k=1,k\neq i}^{N} f_{zk}^{i}(\boldsymbol{X}) \end{cases} \tag{11}$$

where e, θ are eccentricity and true anomaly of the CM orbit. The denotation of $[\,]'$ represents the derivative with respect to θ and the relationship with respect to the time derivative is derived as

$$\begin{cases} \dfrac{d}{dt} = \dot{\theta}\dfrac{d}{d\theta} \\ \dfrac{d^2}{dt^2} = \dot{\theta}^2\dfrac{d^2}{d\theta^2} + \ddot{\theta}\dfrac{d}{d\theta} \end{cases} \tag{12}$$

where $\dot{\theta}, \ddot{\theta}$ are calculated as

$$\dot{\theta} = \frac{n_{\mathrm{CM}}(1+e\cos\theta)^2}{(1-e^2)^{3/2}}$$

and

$$\ddot{\theta} = \frac{-2n_{\mathrm{CM}}^2 e\sin\theta(1+e\cos\theta)^3}{(1-e^2)^3}.$$

The dynamic model of relative motion for satellite j with respect to satellite i can be similarly derived as Eq. (10).

3) CM with general Keplerian orbit.

When CM with general Keplerian orbit is assumed, the derivative equations of orbit elements can be utilized [20]. For eliminating the singularities of $i = 0$ and $e = 0$, the modified equinoctial elements $\boldsymbol{\sigma}_i = [\ p_i\ \ f_i\ \ g_i\ \ h_i\ \ k_i\ \ L_i\ ]^{\mathrm{T}}$ are used to denote the absolute position/velocity vector of satellite i. The relationships between the modified equinoctial and the classical orbit elements are defined as

$$\begin{cases} p = a(1-e^2), \quad f = e\cos(\omega+\Omega), \quad g = e\sin(\omega+\Omega) \\ h = \tan(i/2)\cos\Omega, \quad k = \tan(i/2)\sin\Omega, \quad L = \Omega+\omega+\theta \end{cases} \tag{13}$$

where a is semi-major axis, i the inclination and ω the argument of perigee.

The derivative equations of the modified equinoctial elements for satellite i with inter-satellite non-contacting force are given as

$$\dot{\boldsymbol{\sigma}}_i = \boldsymbol{A}(\boldsymbol{\sigma}_i)\sum_{k=1,k\neq i}^{n}\boldsymbol{f}_k^i + \boldsymbol{B}(\boldsymbol{\sigma}_i) \tag{14}$$

where matrices $\boldsymbol{A}(\boldsymbol{\sigma}_i)$ and $\boldsymbol{B}(\boldsymbol{\sigma}_i)$ are defined as reference [20].

Considering the idealized case of mere existence of gravitational force and inter-satellite non-contacting actuations, the derivatives of orbit elements of CM are zero and the derivatives of the relative orbit elements are derived as

$$\begin{cases} \delta\dot{\boldsymbol{\sigma}}_{i\mathrm{CM}} = [\ \dot{p}_i \quad \dot{f}_i \quad \dot{g}_i \quad \dot{h}_i \quad \dot{k}_i \quad \dot{L}_i\ ]^{\mathrm{T}} \\ \delta\dot{\boldsymbol{\sigma}}_{ij} = [\ \dot{p}_i-\dot{p}_j \quad \dot{f}_i-\dot{f}_j \quad \dot{g}_i-\dot{g}_j \quad \dot{h}_i-\dot{h}_j \quad \dot{k}_i-\dot{k}_j \quad \dot{L}_i-\dot{L}_j\ ]^{\mathrm{T}} \end{cases} \tag{15}$$

Therefore, based on Eqs. (14) and (15), the dynamic models of relative motions between satellite i and CM, satellite i and j, can be directly derived.

2.3. Dynamic model of relative attitude motion

Assuming that all the satellites are spherical symmetry and based on the Euler equations [21], the relative attitude dynamic model of satellite i is derived as

$$\begin{cases} I_{xi}\dot{\omega}_{xi} + (I_{zi}-I_{yi})\omega_{yi}(\omega_{zi}+\dot{\theta}) = \sum\limits_{k=1,k\neq i}^{n}\tau_{xk}^{i}(\boldsymbol{X}) \\ I_{yi}\dot{\omega}_{yi} + (I_{xi}-I_{zi})\omega_{xi}(\omega_{zi}+\dot{\theta}) = \sum\limits_{k=1,k\neq i}^{n}\tau_{yk}^{i}(\boldsymbol{X}) \\ I_{zi}(\dot{\omega}_{zi}+\ddot{\theta}) + (I_{yi}-I_{xi})\omega_{xi}\omega_{yi} = \sum\limits_{k=1,k\neq i}^{n}\tau_{zk}^{i}(\boldsymbol{X}) \end{cases} \tag{16}$$

where $(\omega_{xi}, \omega_{yi}, \omega_{zi})$ are the angular velocities projected at and with respect to the Hill frame at CM, and $(\tau_{xk}^i, \tau_{yk}^i, \tau_{zk}^i)$ the magnetic torques.

3. Dynamics analysis

Although the electrostatic force, the electromagnetic force and the magnetic flux-pinned force have significant differences in producing mechanism, effective actuation distance, effects to translational and rotational motions, summarized as Table 1, they share similar essential properties of internal, non-contacting and simultaneous actuation, which highlight some special constraints of relative motion dynamics and interesting dynamics characteristics when applied to the near-Earth relative orbit motion and the deep space relative motion.

3.1. Constraints of relative motion dynamics

The inter-satellite non-contacting force is a kind of cluster internal force, which satisfies

$$\boldsymbol{F}_k^i = -\boldsymbol{F}_i^k \tag{17}$$

Therefore, the sum of all the inter-satellite non-contacting forces for the spacecraft cluster satisfies

$$\sum_{k=1}^{N}\sum_{i=1,i\neq k}^{N}\boldsymbol{F}_i^k = \boldsymbol{0} \tag{18}$$

Table 1
Differences of the three inter-satellite non-contacting forces.

	Electrostatic force	Electromagnetic force	Magnetic flux-pinned force
Producing mechanism	Coulomb law	Biot–Savart law	Special property of the superconductor
Effective actuation distance	$F \sim 1/r^2$	$F \sim 1/r^4$	$F \sim 1/r^4$
Effects to translational and rotational motions	Generally affect translational motion	Affect translational and rotational motions	Affect translational and rotational motions

Additionally, both this generic force and torque cannot change the total angular momentum of the cluster with respect to any reference point, indicating that the corresponding total torque is zero. Taking the CM as reference point, the total torque brought by the inter-satellite non-contacting force satisfies

$$\sum_{i=1}^{N}\left(\boldsymbol{r}_i \times \sum_{k=1,k\neq i}^{N} \boldsymbol{F}_k^i + \boldsymbol{\tau}_i\right) = \boldsymbol{0} \tag{19}$$

where $\boldsymbol{\tau}_i$ is the magnetic torque vector.

Considering the above analyzed characteristics of inter-satellite non-contacting force and torque, the spacecraft cluster essentially has constraints as to its relative motion dynamics: conservation of the total angular momentum vector and the total mechanical energy. Combining these conservations with the definition of CM, it can be seen that seven scalar constraints exist.

Firstly, corresponding to the definition of CM, the relative distance and velocity vectors satisfy

$$\begin{cases} \sum_{i=1}^{N} m_i \boldsymbol{r}_i = \boldsymbol{0} \\ \sum_{i=1}^{N} m_i \dfrac{d\boldsymbol{r}_i}{dt} = \sum_{i=1}^{N} m_i(\dot{\boldsymbol{r}}_i + n_{\mathrm{CM}} \times \boldsymbol{r}_i) \\ \qquad = \sum_{i=1}^{N} m_i \dot{\boldsymbol{r}}_i + n_{\mathrm{CM}} \times \sum_{i=1}^{N} m_i \boldsymbol{r}_i = \sum_{i=1}^{N} m_i \dot{\boldsymbol{r}}_i = \boldsymbol{0} \end{cases} \tag{20}$$

where m_i is the mass and $\dot{\boldsymbol{r}}_i$ the relative velocity vector with respect to the Hill frame at CM.

Secondly, consider the idealized case that only the inter-satellite non-contacting force and the Earth's gravitational force be exploited, where the former one is cluster internal force and the latter one is collinear with the distance vector of satellite with respect to the Earth's center. Therefore, the total angular momentum of the spacecraft cluster with respect to the Earth's center is conserved and expressed as

$$\boldsymbol{H}_{\mathrm{E}} = \sum_{i=1}^{N} \boldsymbol{R}_i \times m_i \dot{\boldsymbol{R}}_i = \text{Constant vector} \tag{21}$$

Substituting $\boldsymbol{R}_i = \boldsymbol{R}_{\mathrm{CM}} + \boldsymbol{r}_i$ into Eq. (21), the constraints of relative motion dynamics for the conservation of total angular momentum are derived as

$$\begin{aligned} \boldsymbol{H}_{\mathrm{E}} &= M\boldsymbol{R}_{\mathrm{CM}} \times \dot{\boldsymbol{R}}_{\mathrm{CM}} + \sum_{i=1}^{N} m_i \boldsymbol{r}_i \times \frac{d\boldsymbol{r}_i}{dt} \\ &= M\boldsymbol{R}_{\mathrm{CM}} \times \dot{\boldsymbol{R}}_{\mathrm{CM}} + \boldsymbol{H}_{\mathrm{CM}} = \text{Constant vector} \\ &\Rightarrow \quad \sum_{i=1}^{N} m_i \boldsymbol{r}_i \times \frac{d^2\boldsymbol{r}_i}{dt^2} + M\boldsymbol{R}_{\mathrm{CM}} \times \ddot{\boldsymbol{R}}_{\mathrm{CM}} = \boldsymbol{0} \end{aligned} \tag{22}$$

where M is the total mass of the spacecraft cluster and $\boldsymbol{H}_{\mathrm{CM}}$ the total angular momentum vector with respect to CM.

Thirdly, because the Earth's gravitational force and the inter-satellite non-contacting force belong to the generic conservative force, so the total mechanical energy of the spacecraft cluster is conserved and derived as

$$\sum_{i=1}^{N}\left(\frac{1}{2} m_i \dot{\boldsymbol{R}}_i \cdot \dot{\boldsymbol{R}}_i - \mu_{\mathrm{E}} \frac{m_i}{R_i} + P_i(\boldsymbol{r}_{ij})\right) = \text{Constant} \tag{23}$$

where μ_{E} is the Earth's gravitational constant and $P_i(\boldsymbol{r}_{ij})$ the potential energy resulted by the inter-satellite actuation fields.

Substituting $\boldsymbol{R}_i = \boldsymbol{R}_{\mathrm{CM}} + \boldsymbol{r}_i$ into Eq. (23), the constraints of relative motion dynamics for the conservation of total mechanical energy can be expressed as the nonlinear function of the variables R_{CM}, r_i and r_{ij}.

With the above analysis, it can be concluded that the definition of cluster center of mass exerts three constraints to the relative positions, while the conservations of the total angular momentum and the total mechanical energy exert four constraints to the coupled dynamics of the absolute orbit motion of CM and the relative motion of every satellite.

3.2. Characteristics of application to near-Earth relative orbit motion

These three inter-satellite non-contacting forces may enable many near-Earth space missions to be accomplished from a novel viewpoint, such as rendezvous and docking, large space structure on-orbit assembly, and failure satellite re-orbiting or de-orbiting operations. However, as to the applications of these forces to the near-Earth relative orbit motion, the effects of the Earth's gravitational field make the dynamics complex.

Considering the effects of the Earth's gravitational field, the equivalent vector equations of motion can be derived as

$$\begin{cases} \boldsymbol{F}_{\mathrm{IN1}} - \boldsymbol{F}_{\mathrm{des1}} - \boldsymbol{F}_{\mathrm{GE1}} = \boldsymbol{0} \\ \boldsymbol{F}_{\mathrm{IN2}} - \boldsymbol{F}_{\mathrm{des2}} - \boldsymbol{F}_{\mathrm{GE2}} = \boldsymbol{0} \\ \quad \vdots \\ \boldsymbol{F}_{\mathrm{INN-1}} - \boldsymbol{F}_{\mathrm{desN-1}} - \boldsymbol{F}_{\mathrm{GEN-1}} = \boldsymbol{0} \\ \boldsymbol{F}_{\mathrm{INN}} - \boldsymbol{F}_{\mathrm{desN}} - \boldsymbol{F}_{\mathrm{GEN}} = \boldsymbol{0} \end{cases} \tag{24}$$

where subscript "IN" denotes the "Inter-satellite Non-contacting" term, "des" the desired term and "GE" the Earth's gravitational term.

Because of the actuation of the Earth's gravitational field, we can find that the complex of the solution for the corresponding control variables increases from analysis of Eq. (24). And then, considering the constraints of Eq. (18), it can be seen that the degrees of freedom of the cluster including n satellites is $3(n-1)$. As for the electrostatic force, the number of control variables is n. As for the electromagnetic force, the number is $3n$ and the number for magnetic flux-pinned force is $3(n-1)$. Therefore, we put forward that the solution of control variables for the magnetic flux-pinned force is unique, yet multiple for the electromagnetic force. However, as to the electrostatic force, in order to generating a feasible solution, some special dynamics constraints need be added [22].

In addition, three operational considerations should be emphasized. Firstly, due to the inverse relationship of two times or four times between the inter-satellite non-contacting force and the inter-satellite distance, its application should be in very closely

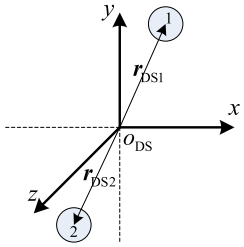

Fig. 4. Inertial coordinate frame at CM for deep space operation.

spaced clusters. Secondly, whenever a satellite activates its electromagnet in LEO, a disturbance force and torque would be produced on it due to the Earth's magnetic field. Therefore, when electromagnetic force or magnetic flux-pinned force applies, the effects of the Earth's magnetic field cannot be neglected. Thirdly, considering the Debye shielding effect, the electrostatic force must apply to higher altitude orbits, such as GEO.

3.3. Characteristics of application to deep space relative motion

Deep space may be a main research and application field of this generic inter-satellite non-contacting force, which is the only force actuated. Furthermore, the orbit motion with respect to a large gravitational body does not exist and only the relative motion between these spacecraft survives.

1) Several special dynamics characteristics.

When the generic inter-satellite non-contacting force is applied to deep space missions, the total linear momentum $\boldsymbol{L}$ and the absolute motion of CM are conserved, which can be expressed as

$$\begin{cases} \boldsymbol{L} = \sum_{i=1}^{N} m_i \boldsymbol{v}_i = \text{Constant vector} \\ M\boldsymbol{r}_{\text{CM}} = \boldsymbol{A}t + \boldsymbol{B} \end{cases} \tag{25}$$

where $\boldsymbol{v}_i$ is the inertial velocity vector with respect to CM and $\boldsymbol{r}_{\text{CM}}$ the inertial position vector of CM. And, $\boldsymbol{A}$ and $\boldsymbol{B}$ are two arbitrary constant matrices.

In addition, the total angular momentum of this deep space application with respect to CM is conserved and derived as Eq. (26), which is different from the non-conservation Eq. (22) with additional actuation of the gravitational force.

$$\boldsymbol{H}_{\text{CM}} = \sum_{i=1}^{N} (\boldsymbol{I}_i \boldsymbol{\omega}_i + m_i \boldsymbol{r}_i \times \boldsymbol{v}_i) = \text{Constant vector} \tag{26}$$

where $\boldsymbol{r}_i$ is the inertial position vector with respect to CM and $\boldsymbol{\omega}_i$ the inertial angular velocity.

2) Artificial relative orbit motion.

As to the two-spacecraft cluster deep space operations with the generic inter-satellite non-contacting force, an "artificial relative orbit motion" similar to that enabled by the gravitational force may be realized. Developing the reference coordinate frame $o_{\text{DS}}xyz$ as Fig. 4, with its origin at CM, the relative distance vector $\boldsymbol{d}_{\text{DS12}}$ from satellite 1 to satellite 2 is derived as $\boldsymbol{d}_{\text{DS12}} = \boldsymbol{r}_{\text{DS2}} - \boldsymbol{r}_{\text{DS1}}$.

Taking the close proximity electrostatic formation for example, the relative motion dynamic model of this two-spacecraft cluster is derived as

$$\begin{aligned} \ddot{\boldsymbol{d}}_{\text{DS12}} &= \ddot{\boldsymbol{r}}_{\text{DS2}} - \ddot{\boldsymbol{r}}_{\text{DS1}} = \frac{k_c}{m_2} \frac{\boldsymbol{r}_{\text{DS2}} - \boldsymbol{r}_{\text{DS1}}}{d_{\text{DS12}}^3} q_1 q_2 \\ &\quad - \frac{k_c}{m_1} \frac{\boldsymbol{r}_{\text{DS1}} - \boldsymbol{r}_{\text{DS2}}}{d_{\text{DS12}}^3} q_1 q_2 \\ &= \frac{k_c q_1 q_2}{d_{\text{DS12}}^3} \left(\frac{\boldsymbol{r}_{\text{DS2}} - \boldsymbol{r}_{\text{DS1}}}{m_2} - \frac{\boldsymbol{r}_{\text{DS1}} - \boldsymbol{r}_{\text{DS2}}}{m_1} \right) \end{aligned} \tag{27}$$

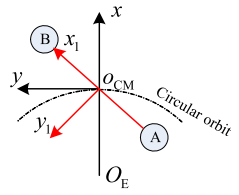

Fig. 5. Schematic drawing of the co-rotating pair satellites.

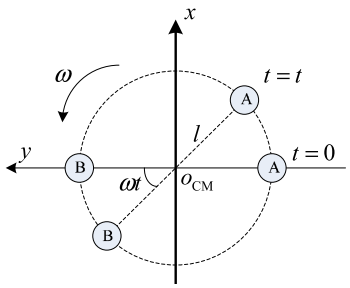

Fig. 6. Desired relative positions of the co-rotating pair satellites.

Applying the definition of $\boldsymbol{d}_{\text{DS12}}$ into Eq. (27), the dynamic model is simplified as

$$\ddot{\boldsymbol{d}}_{\text{DS12}} = \frac{k_c q_1 q_2}{d_{\text{DS12}}^3} \frac{m_1 + m_2}{m_1 m_2} \boldsymbol{d}_{\text{DS12}} \quad \Rightarrow \quad \ddot{\boldsymbol{d}}_{\text{DS12}} + \frac{\mu_{\text{ES}}}{d_{\text{DS12}}^2} \hat{\boldsymbol{d}}_{\text{DS12}} = \boldsymbol{0} \tag{28}$$

where $\mu_{\text{ES}} = -k_c q_1 q_2 (m_1 + m_2)/m_1 m_2$ is the controllable parameter similar to the gravitational constant.

Similar to the two-body problem of the celestial dynamics, from analysis of Eq. (28) it can be known that the relative motion of satellite 2 with respect to satellite 1 in the two-spacecraft electrostatic cluster is a kind of conic-section curve. Therefore, this "artificial relative orbit motion" could also be described by six integration constants, and many of the related characteristics would be investigated in the near future.

When more satellites are included into the spacecraft cluster, or the other two forces are considered, the above interesting "artificial relative orbit motion" could not be ensured. However, the corresponding characteristics of dynamics could be similar analyzed as the celestial dynamics with multiple-gravitational forces.

4. Simulation analysis

In this section, a CM orbital coplanar co-rotating pair satellites case was utilized to verify the feasibility of this unified modeling approach, the control capability and dynamics characteristics. The absolute motion of the CM is assumed a circular orbit, depicted as Fig. 5, where $o_{\text{CM}}xy$ is portion of the Hill frame and $o_{\text{CM}}x_1y_1$ the co-rotating pair body frame. And then, a related deep space application case was also exploited.

The dynamic model is derived as

$$\begin{cases} \ddot{x}_{\text{B}} - 2n_{\text{CM}}\dot{y}_{\text{B}} - 3n_{\text{CM}}^2 x_{\text{B}} = f_{\text{B}x} \\ \ddot{y}_{\text{B}} + 2n_{\text{CM}}\dot{x}_{\text{B}} = f_{\text{B}y} \end{cases} \tag{29}$$

where $[x_{\text{B}}, y_{\text{B}}, \dot{x}_{\text{B}}, \dot{y}_{\text{B}}]^{\text{T}}$ are relative positions/velocities of satellite B with respect to the Hill frame at CM, and $[f_{\text{B}x}, f_{\text{B}y}]^{\text{T}}$ are the Hill frame projected specific forces actuated on satellite B.

The desired relative positions could be solved from Fig. 6, where l and ω are the rotation radius and angular speed, respectively. The initial motion states with respect to the Hill frame are set as Eq. (30) and the simulation parameter values are as Table 2.

Table 2
Simulation parameters.

Parameter	Value	Parameter	Value	Parameter	Value
CM orbit height	36 000 km	r_{FC}	0.1 m	μ_{FC}	1000 Am^2
m	50 kg	l	5 m	ω	$200 \times n_{CM}$

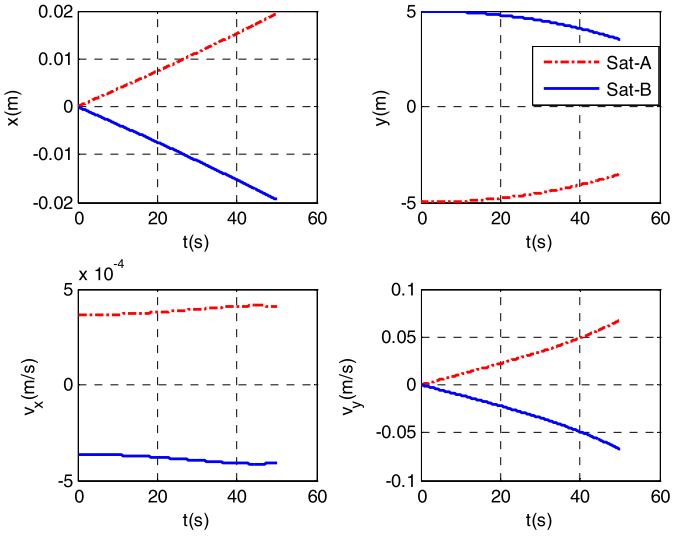

Fig. 7. Relative positions and velocities of the co-rotating pair actuated by electrostatic force.

$$\begin{cases} x_A = 0, \quad y_A = -5\ \text{m}, \quad \dot{x}_A = 5\pi/43\,200\ (\text{m/s}), \quad \dot{y}_A = 0 \\ x_B = 0, \quad y_B = 5\ \text{m}, \quad \dot{x}_B = -5\pi/43\,200\ (\text{m/s}), \quad \dot{y}_B = 0 \end{cases} \tag{30}$$

Based on these above settings, following gives the simulation results for the electrostatic force, the electromagnetic force and the magnetic flux-pinned force, respectively.

1) Electrostatic force.

The specific electrostatic forces are derived as

$$\begin{bmatrix} f_{Bx} \\ f_{By} \end{bmatrix} = -\frac{k_c q_A q_B}{4m(x_B^2 + y_B^2)^{1.5}} \begin{bmatrix} x_B \\ y_B \end{bmatrix} \tag{31}$$

Eq. (31) satisfies $f_{Bx}/f_{By} = x_B/y_B$. However, from Eq. (29) it can know that $f_{Bx}/f_{By} \neq x_B/y_B$ generally exists. Therefore, it can be safely put forward that applying only electrostatic force couldn't realize this co-rotating pair. Nevertheless, the relative motion still satisfies the definition of CM and several conservations, which can be directly deduced from Fig. 7. In addition, the angular momentum with respect to CM is also given as Fig. 8, from which it can be seen that this angular momentum isn't conserved, consistent with the theoretical deduction.

2) Electromagnetic force.

The electrostatic formulation of the electromagnetic force is depicted as Fig. 9.

Because only two translational degrees-of-freedom need to be controlled, $\alpha = 0$ and $\mu_A = 1.0 \times 10^5$ (Am^2) are set, then the specific far-field electromagnetic force model is simplified as

$$\begin{bmatrix} f_{Bx} \\ f_{By} \end{bmatrix} = \frac{3}{64\pi} \frac{\mu_0 \mu_A \mu_B}{m(x_B^2 + y_B^2)^{2.5}} \begin{bmatrix} -2\cos\beta x_B - \sin\beta y_B \\ -2\cos\beta y_B + \sin\beta x_B \end{bmatrix} \tag{32}$$

The desired specific control forces are derived from Fig. 6 as

$$f_{B\_desire} = l \begin{bmatrix} \omega^2 \sin(\omega t) + 2n_{CM}\omega \sin(\omega t) + 3n_{CM}^2 \sin(\omega t) \\ -\omega^2 \cos(\omega t) - 2n_{CM}\omega \cos(\omega t) \end{bmatrix} \tag{33}$$

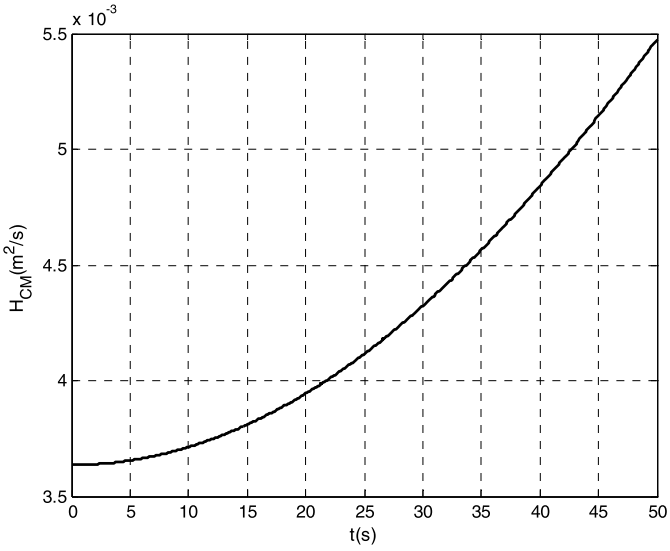

Fig. 8. Angular momentum with respect to CM.

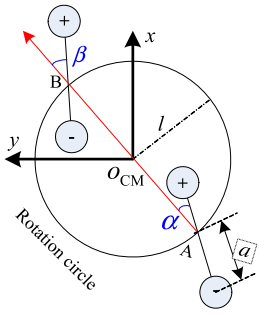

Fig. 9. Electrostatic schematic drawing of the electromagnetic force.

By equaling Eqs. (32) and (33), the desired control variables could be solved and depicted as Fig. 10.

For verifying the electrostatic formulation of the electromagnetic force, without loss of generality, the one-dimensional mathematical models of Eqs. (34) and (35) are exploited and compared as Fig. 11, from which it can be known that the two formulations of electromagnetic force are equivalent.

$$\begin{bmatrix} f_{Bx} \\ f_{By} \end{bmatrix} = -\frac{3}{32\pi} \frac{\mu_0 \mu_A \mu_B}{m(x_B^2 + y_B^2)^{2.5}} \begin{bmatrix} x_B \\ y_B \end{bmatrix} \tag{34}$$

$$\begin{bmatrix} f_{Bx} \\ f_{By} \end{bmatrix}_{ES} = \frac{1}{m}\left(\frac{k_c q_A q_B}{2(x_B^2 + y_B^2)^{1.5}} - \frac{1}{4}\left(\frac{k_c q_A q_B}{((x_B^2 + y_B^2)^{0.5} + a)^2} + \frac{k_c q_A q_B}{((x_B^2 + y_B^2)^{0.5} - a)^2} \right) \frac{1}{(x_B^2 + y_B^2)^{0.5}} \right) \begin{bmatrix} x_B \\ y_B \end{bmatrix} \tag{35}$$

3) Magnetic flux-pinned force

The electrostatic formulation of the magnetic flux-pinned force is depicted as Fig. 12, and the magnetic flux-pinned force of which could be derived as Eqs. (36)–(38).

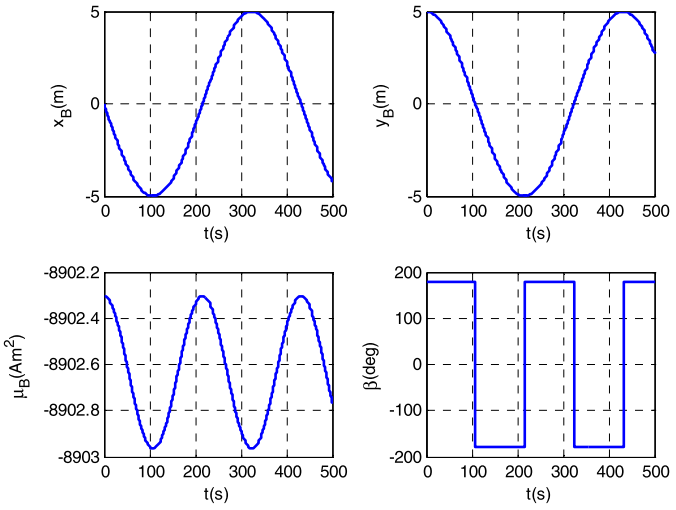

Fig. 10. Relative positions and solutions of control variables.

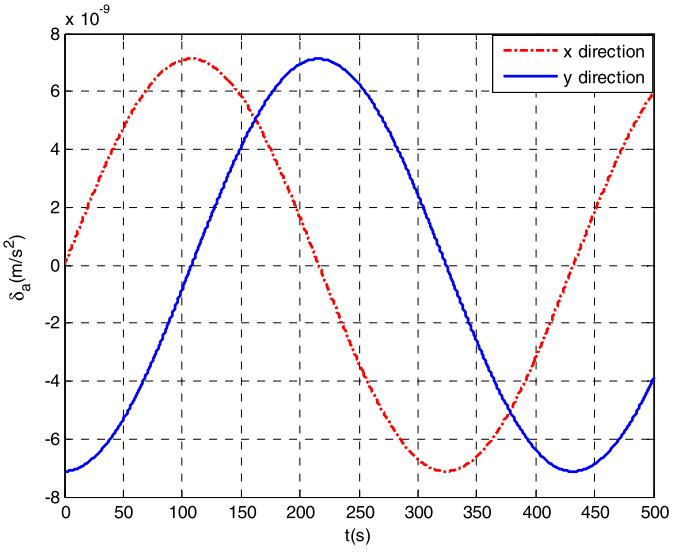

Fig. 11. Deviation between electromagnetic force and its corresponding electrostatic formulation.

$$\begin{bmatrix} f_{Bx} \\ f_{By} \end{bmatrix}_{\text{Frozen}} = \frac{3}{4\pi} \frac{\mu_0 \mu_A \mu_B}{m((x_B^2+y_B^2)^{0.5}+r_{FC})^4 (x_B^2+y_B^2)^{0.5}} \times \begin{bmatrix} -2\cos\beta x_B - \sin\beta y_B \\ -2\cos\beta y_B + \sin\beta x_B \end{bmatrix} \begin{bmatrix} x_B \\ y_B \end{bmatrix} \tag{36}$$

$$\begin{bmatrix} f_{Bx} \\ f_{By} \end{bmatrix}_{\text{Mobile}} = \frac{3}{64\pi} \frac{\mu_0 \mu_B^2 (1+\cos^2\beta)}{m(x_B^2+y_B^2)^{2.5}} \begin{bmatrix} x_B \\ y_B \end{bmatrix} \tag{37}$$

$$\begin{bmatrix} f_{Bx} & f_{By} \end{bmatrix}^T = \begin{bmatrix} f_{Bx} & f_{By} \end{bmatrix}^T_{\text{Frozen}} + \begin{bmatrix} f_{Bx} & f_{By} \end{bmatrix}^T_{\text{Mobile}} \tag{38}$$

By equaling Eqs. (33) and (38), the desired control variables could be similar solved as the electromagnetic force case.

For verifying the electrostatic formulation of the magnetic flux-pinned force, without loss of generality, the one-dimensional mathematical models of Eqs. (39) and (40) are exploited and compared as Fig. 13, from which it can be known that the two formulations of magnetic flux-pinned force are equivalent.

$$\begin{bmatrix} f_{Bx} \\ f_{By} \end{bmatrix} = \left(-\frac{3}{2\pi} \frac{\mu_0 \mu_A \mu_B}{m((x_B^2+y_B^2)^{0.5}+r_{FC})^4 (x_B^2+y_B^2)^{0.5}} + \frac{3}{32\pi} \frac{\mu_0 \mu_B^2}{m(x_B^2+y_B^2)^{2.5}} \right) \begin{bmatrix} x_B \\ y_B \end{bmatrix} \tag{39}$$

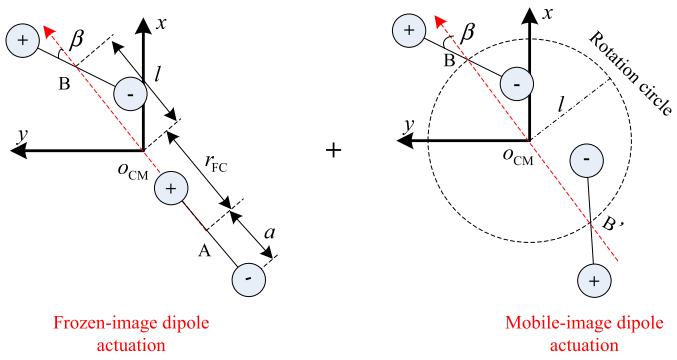

Fig. 12. Electrostatic schematic drawing of the magnetic flux-pinned force.

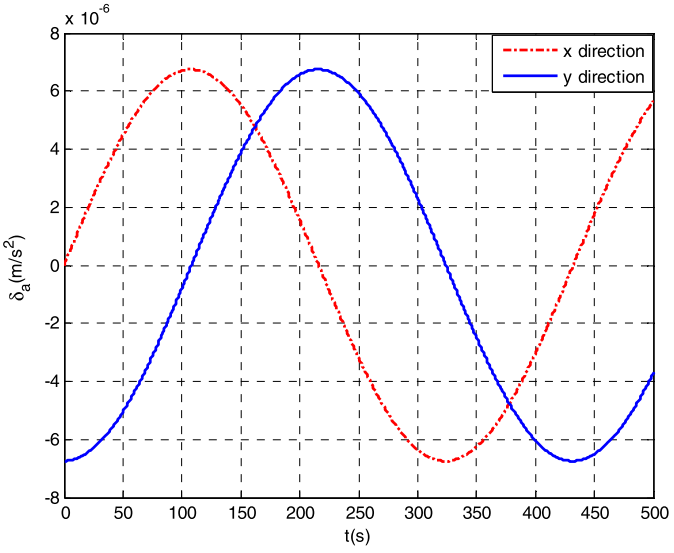

Fig. 13. Deviation between magnetic flux-pinned force and its corresponding electrostatic formulation.

$$\begin{aligned} \begin{bmatrix} f_{Bx} \\ f_{By} \end{bmatrix}_{ES} = \frac{1}{m} \Bigg(& \frac{-k_c q_B^2}{2(x_B^2+y_B^2)^{1.5}} + \frac{1}{4} \Bigg(\frac{k_c q_B^2}{((x_B^2+y_B^2)^{0.5}+a)^2} \\ & + \frac{k_c q_B^2}{((x_B^2+y_B^2)^{0.5}-a)^2} \Bigg) \frac{1}{(x_B^2+y_B^2)^{0.5}} \Bigg) \begin{bmatrix} x_B \\ y_B \end{bmatrix} \\ & + \Bigg(\frac{2k_c q_{FC} q_B}{((x_B^2+y_B^2)^{0.5}+r_{FC})^2} \\ & - \Bigg(\frac{k_c q_{FC} q_B}{((x_B^2+y_B^2)^{0.5}+r_{FC}+2a)^2} \\ & + \frac{k_c q_{FC} q_B}{((x_B^2+y_B^2)^{0.5}+r_{FC}-2a)^2} \Bigg) \Bigg) \\ & \times \frac{1}{m(x_B^2+y_B^2)^{0.5}} \begin{bmatrix} x_B \\ y_B \end{bmatrix} \end{aligned} \tag{40}$$

In addition, a case of two electrostatic spacecraft cluster in deep space was exploited to further verify the several characteristics: conservations of the total linear momentum and the total angular momentum. The related simulation parameters are set consistent with the above cases and the results are depicted as Fig. 14, from which the conservations could be seen.

5. Conclusions

Based on the theoretical derivations and numerical verifications for dynamic models and dynamics of spacecraft relative motion

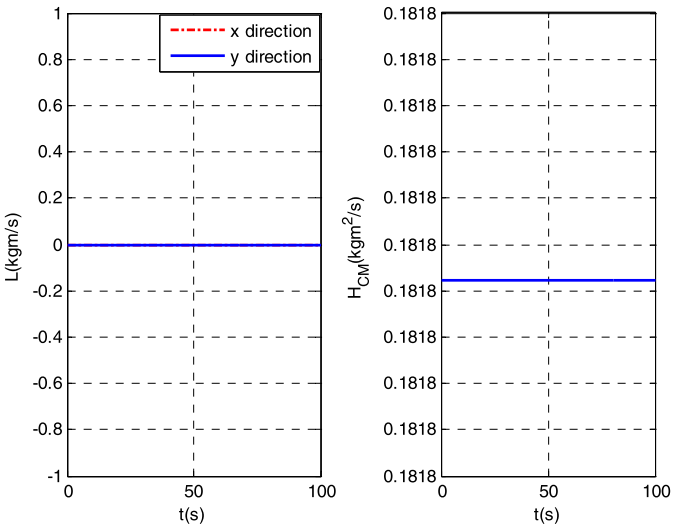

Fig. 14. Linear and angular momentum with respect to CM for deep space electrostatic spacecraft cluster.

actuated by inter-satellite non-contacting forces, some useful and interesting conclusions can be safely put forward. Firstly, utilizing the electrostatic/magnetostatic duality theorem and the two dipole representation of the magnetic flux-pinned actuation, the mathematical models of the electrostatic force, the electromagnetic force and the magnetic flux-pinned force can be unified modeling. Secondly, based on the Hill frame at the center of mass (denoted as CM) of the spacecraft cluster, by exploiting the Hill equations, the T–H equations and the derivative equations of modified equinoctial elements, the dynamic models of spacecraft relative motion considering different level assumptions can be directly derived. Thirdly, the actuation of this inter-satellite non-contacting force highlights several constraints of the coupled dynamics containing the absolute orbit motion of the CM and the relative motion of every satellite. Specifically, when applied to the near-Earth relative orbit mission, the gravitational field of the Earth brings increasing complexity to the control variable solving and should be emphasized treated. And, when applied to the deep space relative motion, the total linear momentum and the absolute motion of the CM further conserve, and an "artificial relative orbit motion" of the two-spacecraft electrostatic cluster exists.

Conflict of interest statement

We declare that we have no conflict of interest.

Acknowledgements

The authors would like to acknowledge their colleague Ms. PENG Wangqiong for her revising suggestions in the paper's English writing, and the anonymous reviewers' comments for every versions of the paper. Additionally, this work is supported in part by a grant from the National Natural Science Foundation of China (11172322).

References

[1] Robert J. McKay, Malcolm Macdonald, James Biggs, Colin McInnes, Survey of highly non-Keplerian orbits with low-thrust propulsion, J. Guid. Control Dyn. 34 (3) (2011) 645–666.
[2] Katsusya Nakanishi, Hirohisa Kojima, Takeo Watanabe, Trajectories of in-plane periodic solutions of tethered satellite system projected on van der Pol planes, Acta Astronaut. 68 (2011) 1024–1030.
[3] Hirohisa Kojima, Hiroki Iwashima, Pavel M. Trivailo, Libration synchronization control of clustered electrodynamic tether system using Kuramoto model, J. Guid. Control Dyn. 34 (3) (2011) 706–718.
[4] Shuquan Wang, Hanspeter Schaub, Coulomb control of nonequilibrium fixed shape triangular three-vehicle cluster, J. Guid. Control Dyn. 34 (1) (2011) 259–270.
[5] Umair Ahsun, David W. Miller, Jaime L. Ramirez, Control of electromagnetic satellite formations in near-Earth orbits, J. Guid. Control Dyn. 33 (6) (2010) 1883–1891.
[6] Michael C. Norman, Mason A. Peck, Simplified model of a magnetic flux-pinned spacecraft formation, J. Guid. Control Dyn. 33 (3) (2010) 814–822.
[7] Young K. Bae, Photonic laser propulsion (PLP): photon propulsion using an active resonant optical cavity, in: Proceedings of the 2007 AIAA Space Conference and Exposition, September 18–20, Long Beach, CA, 2007.
[8] Samuel A. Schweighart, Raymond J. Sedwick, Electromagnetic Formation Flight Dipole Solution Planning, Massachusetts Institute of Technology, MA, 2005.
[9] William R. Wilson, Joseph P. Shoer, Mason A. Peck, Demonstration of a magnetic locking magnetic flux-pinned revolute joint for use on cubesat-standard spacecraft, in: AIAA Guidance, Navigation, and Control Conference, 10–13 August 2009, Chicago, IL, 2009, pp. 1–13.
[10] Laura L. Jones, Mason A. Peck, Stability and control of a magnetic flux-pinned docking interface for spacecraft, in: AIAA Guidance, Navigation, and Control Conference, 2–5 August 2010, Toronto, Ontario, Canada, 2010, pp. 1–12.
[11] W.H. Clohessy, R.S. Wiltshire, Terminal guidance system for satellite rendezvous, J. Aerosp. Sci. 27 (9) (1960) 653–658.
[12] Erik A. Hogan, Hanspeter Schaub, Linear stability and shape analysis of spinning three-craft Coulomb formations, Celest. Mech. Dyn. Astron. 112 (2012) 131–148.
[13] Ahsun Umair, David W. Miller, Dynamics and control of electromagnetic satellite formations, in: Proceedings of the 2006 American Control Conference, Minneapolis, MN, June 14–16, 2006, 2007, pp. 1730–1735.
[14] Joseph P. Shoer, Magnetic flux-pinned interfaces for the assembly, manipulation, and reconfiguration of modular space systems, J. Astronaut. Sci. (2010) 1–12.
[15] Michael C. Norman, Mason A. Peck, Orbit maneuvers through inter-satellite forcing, in: AIAA Guidance, Navigation, and Control Conference, 10–13 August 2009, Chicago, IL, 2009.
[16] Michael C. Norman, Mason A. Peck, Integrals of motion for planar multibody formations with internal forces, J. Guid. Control Dyn. 34 (6) (2011) 1790–1797.
[17] A. Kordyuk, Magnetic levitation for hard superconductor, J. Appl. Phys. 83 (1) (1998) 610–612.
[18] Joseph P. Shoer, Mason A. Peck, Reconfigurable spacecraft as kinematic mechanisms based on flux-pinning interactions, J. Spacecr. Rockets 46 (2) (2009) 466–469.
[19] D.J. Zanon, M.E. Campbell, Optimal planner for spacecraft formations in elliptical orbits, J. Guid. Control Dyn. 29 (1) (2006) 161–171.
[20] A. Kluever Craig, Optimal low-thrust interplanetary trajectories by direct method techniques, J. Astronaut. Sci. 45 (3) (1997) 247–262.
[21] Hanspeter Schaub, John L. Junkins, Analytical Mechanics of Space Systems, AIAA Education Series, AIAA, Reston, VA, October 2003.
[22] John J. Berryman, Analytical and Numerical Analysis of Static Coulomb Formations, Virginia Polytechnic Institute and State University, VA, 2005.